



SAKARYA ÜNİVERSİTESİ

# FEN BİLİMLERİ ENSTİTÜSÜ DERGİSİ

Sakarya University Journal of Science  
SAUJS

ISSN 1301-4048 e-ISSN 2147-835X Period Bimonthly Founded 1997 Publisher Sakarya University  
<http://www.saujs.sakarya.edu.tr/>

Title: Development of Finite Element Model for a Special Lead Extrusion Damper

Authors: Ahmet GÜLLÜ, Furkan ÇALIM, Cihan SOYDAN, Ercan YÜKSEL

Received: 2020-10-09 00:00:00

Accepted: 2021-09-03 00:00:00

Article Type: Research Article

Volume: 25

Issue: 5

Month: October

Year: 2021

Pages: 1159-1167

How to cite

Ahmet GÜLLÜ, Furkan ÇALIM, Cihan SOYDAN, Ercan YÜKSEL; (2021), Development of Finite Element Model for a Special Lead Extrusion Damper. Sakarya University Journal of Science, 25(5), 1159-1167, DOI: 10.16984/saufenbilder.808517

Access link

<http://www.saujs.sakarya.edu.tr/en/pub/issue/65589/808517>

New submission to SAUJS

<http://dergipark.gov.tr/journal/1115/submission/start>

## Development of Finite Element Model for a Special Lead Extrusion Damper

Ahmet GÜLLÜ\*<sup>1</sup>, Furkan ÇALIM<sup>2</sup>, Cihan SOYDAN<sup>3</sup>, Ercan YÜKSEL<sup>2</sup>

### Abstract

A significant amount of seismic energy is imparted to the structures during earthquakes. The energy spreads within the structure and transforms in various energy forms as dissipated through the structure. The conventional seismic design provides specific ductile regions, namely plastic hinges, on structural elements. Therefore, the energy dissipation capacities of the structural elements and the structure enhance. However, this approach accepts that the deformations will concentrate on the plastic hinge zones and severe damage may occur on structural elements within deformation limits that are defined by the seismic codes. The modern seismic design aims to dissipate a large portion of the seismic input energy by installing energy dissipating devices (*EDDs*) to the structure. Thus, deformation concentrates on *EDDs* which can be replaced after an earthquake, and energy demand for structural elements is decreased. Lead extrusion damper (*LED*) is a passive *EDD* that utilizes the hysteretic behavior of lead. In this paper, the preliminary results of the developed three-dimensional finite element model (*FEM*) for a *LED* is presented. The results obtained from the finite element analysis (*FEA*) were compared with the experimental ones in which *LEDs* were exposed to sinusoidal displacements. Also, the applicability of the developed *FEM* was checked for different component dimensions given in the literature. The comparison study yielded a satisfactory consistency. Additionally, the maximum relative difference obtained for the literature devices was reduced to 12% from 39% by the developed *FEM*.

**Keywords:** Lead extrusion damper, Passive energy dissipater, Seismic energy dissipation, Finite element analysis.

### 1. INTRODUCTION

The energy released during earthquakes imparts to structures. This energy must be dissipated through the structure to prevent life and financial

losses. The conventional seismic design implicitly bases on the principle that structural elements dissipate the imparted energy by various mechanisms and limit displacement and deformation demands for structures. In the

\* Corresponding author: ahmgullu@gmail.com

<sup>1</sup> Istanbul Gedik University

ORCID: <https://orcid.org/0000-0001-6678-9372>

<sup>2</sup> Istanbul Technical University

E-Mail: calimf@itu.edu.tr yukselerc@itu.edu.tr

ORCID: <https://orcid.org/0000-0001-8365-9553>, <https://orcid.org/0000-0002-9741-1206>

<sup>3</sup> Namik Kemal University

E-Mail: csoydan@nku.edu.tr

ORCID: <https://orcid.org/0000-0003-3579-0033>

modern seismic design approach, a large portion of the imparted energy is expected to be dissipated through energy dissipation devices (*EDDs*). Many types of active [1-3] or passive [4-8] *EDDs* were designed and developed in academic and industrial areas to serve this purpose. Additional damping supplied by *EDDs* may reduce inter-story drifts and shear forces through the structure reasonably [9].

Being a soft metal with low yield strength and stiffness makes lead a desirable material for energy dissipation. Hence, it was also utilized in some base isolation systems [10-12]. Lead extrusion damper (*LED*) which is a passive *EDD* also benefits from the metallurgical properties of lead [13-19]. *LED* dissipates the energy by extrusion of lead through a hole or an orifice. The *LED* comprises lead, a tube, a cap, and a bulged shaft, Figure 1.

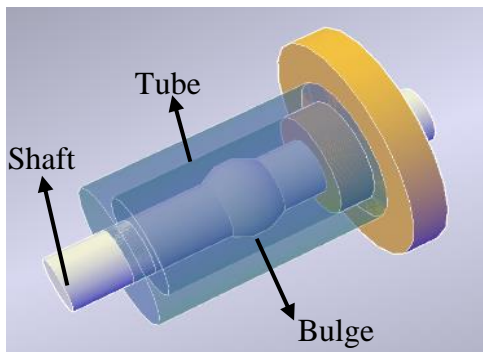


Figure 1 The lead extrusion damper

Even though the behavior of *LED* was determined experimentally in the literature [13-15], the finite element model of the damper is crucial for the prediction of behavior, especially for *LEDs* with distinct geometric dimensions. *LED* is difficult to model by finite elements since lead rapidly gains back its original characteristics, [20]. An effort has been paid on finite element modeling of *LED* by using simplified 2D elements, [21-22].

The rationale of the study is the development of a three-dimensional detailed finite element model of *LEDs* that were tested (*T-LED*), [13-19], and studied in the literature (*L-LED*), [21-22]. To this extent, numerically obtained force-displacement hysteresis of *T-LED* and the maximum force of *L-LED* were compared with the related experimental results.

## 2. MATERIAL AND METHOD

Finite element models of *T-LED* and *L-LED* were generated using the ABAQUS software package, [23].

### 2.1. Performed Experiments on T-LEDs

The *T-LED* was tested under various excitations (e.g. quasi-static, dynamic cyclic, and shaking table tests). The *T-LED* had a bulge on its shaft. The diameters of the bulge and the shaft were 44 and 32 mm, respectively. The surrounding tube had an interior diameter of 60 mm. The tube thickness was 12 mm. The closest distance between the bulge and the tube was 8mm. The displacement capacity of *T-LED* was  $\pm 33$  mm.

Initially, the behavior of *T-LED* was investigated using dynamic tests through sinusoidal excitations with various amplitudes and frequencies, [13]. The experimental setup is shown in Figure 2. It was stated that *T-LED* has almost rectangular load-displacement hysteresis with up to 50% equivalent damping ratio. Additionally, the damping ratio was found to be sensitive to displacement intensity and free from the loading frequency within the adopted displacement and frequency ranges.

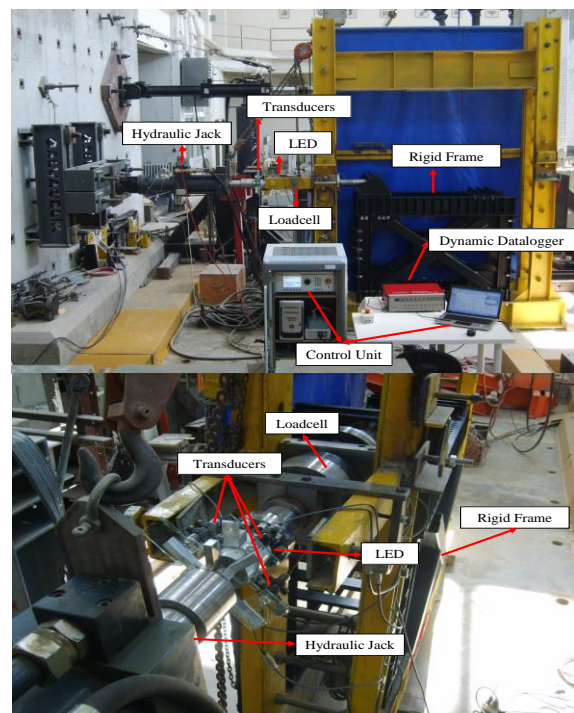


Figure 2 Dynamic tests on the developed *LED*, [13]

Hereafter, *T-LED* was inserted diagonally to a steel beam-to-column connection which was exposed to quasi-static cyclic displacement protocol, Figure 3.



Figure 3 Cyclic steel beam-column connection tests, [14].

The study revealed that the equivalent damping ratio of the connection equipped with *T-LED* was increased up to 6.5 times compared to the bare connection.

Finally, *T-LED* was installed diagonally to the beam-to-column connection of a precast RC frame, [18]. The bare specimen and the specimen equipped with *T-LED* were exposed to real ground motion records on the shake table, Figure 4.

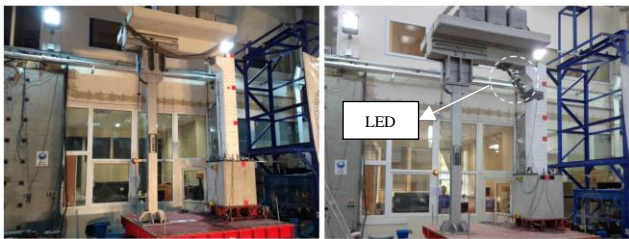


Figure 4 Precast RC beam-column connection shake table tests, [18]

The experimental study resulted that relative top displacement, deformations at the column base, and rotation of the connection joint were reduced up to 50%, 65%, and 30%, respectively by adding *T-LED* to the precast RC frame.

Since the effectiveness of *T-LED* was proven by various tests, a reliable and detailed 3D finite element model was generated to predict the behavioral characteristics of *T-LED* with distinct geometric properties.

## 2.2. Finite Element Model of *T-LED*

In this study, a three-dimensional (3D) finite element model (*FEM*) of *T-LED* was generated, Figure 5. The cap was not modeled for simplicity in the preliminary *FEMs*. Its effect on the behavior of the *T-LED* was considered through boundary conditions. Red, beige and, green parts represent shaft, lead, and tube, respectively, Figure 6.

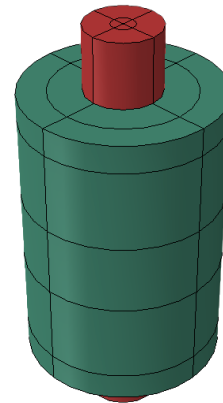


Figure 5 3D finite element model of *T-LED*

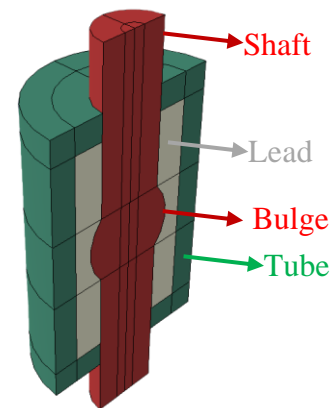


Figure 6 Parts of *T-LED*

An eight-node linear brick, reduced integration elements (C3D8R) were used for all parts of the *LED*. A total number of 33480 mesh elements (14400 elements on the shaft, 9000 elements on the lead, and 10080 elements on the tube) were generated on the instances, Figure 7.

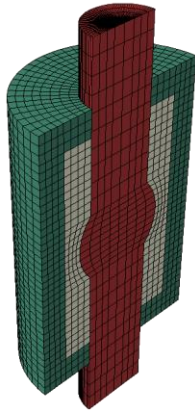
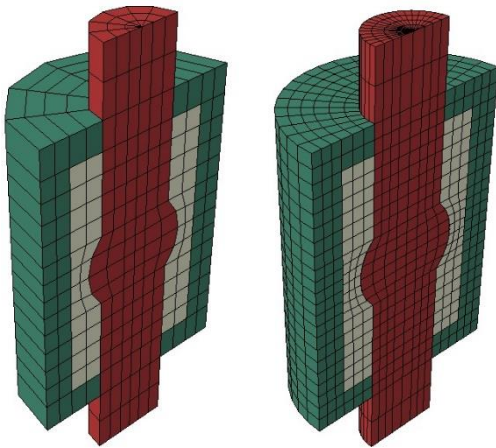


Figure 7 Meshing for FEM of T-LED

A convergence analysis was performed to evaluate the effect of mesh size. In order to serve this purpose, coarse meshing and nearly fine meshing were also applied to the numerical models, Figure 8. In these models, a total of 1320 and 9560 mesh elements were used, respectively.



a) Coarse

b) Nearly fine

Figure 8 Coarse and nearly fine meshing for convergence analyses.

Mechanical properties of the lead, which are available in the literature [21], were used in the preliminary models. The elasticity modulus, Poisson's ratio, and density of the lead were considered as 14 GPa, 0.44, and, 11350 kg/m<sup>3</sup>, respectively.

Surface-to-surface contacts were defined in the models. Contact between lead and steel was modeled by using tangential friction. Analyses were performed by defining a "Static, General" type step. The effects of nonlinearity caused by

both material and geometry are considered in the models.

The movement of the tube was restricted by assigning an encastre (fixed) type boundary condition to both ends of it. A sinusoidal displacement procedure was applied to the shaft, Figure 9. The amplitude of the sinusoidal loadings was 4.5 mm. The consistency of the numerical model was examined by using three cycles for the loading pattern.

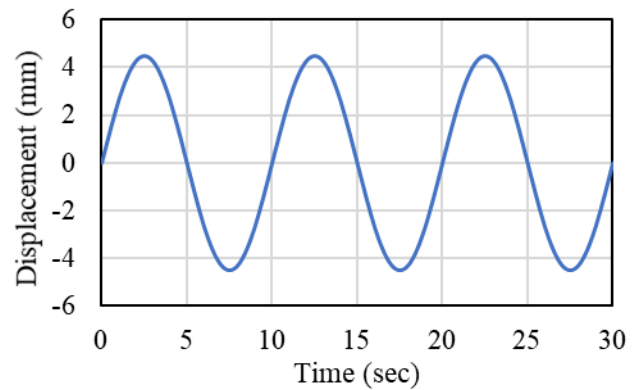


Figure 9 Applied sinusoidal displacement procedure for T-LED

### 2.3. Finite Element Model of L-LEDs

To check the applicability of the developed finite element model on different geometries of LED, FEMs of some selected LED geometries existing in the literature [21, 22] were generated by following the same steps with Chapter 2.2.

Three L-LED geometries with different cylinder, shaft, and bulge diameters ( $D_{cyl}$ ,  $D_{blg}$ ,  $D_{shaft}$ ) and lengths ( $L_{cyl}$ ,  $L_{blg}$ ,  $L_{blgshaft}$ ) were selected, Table 1. The selected geometries belong to the 4<sup>th</sup>, 17<sup>th</sup>, and 19<sup>th</sup> specimens of Vishnupriya [22].

Table 1 Geometric properties of L-LEDs [21, 22]

LED #	$D_{cyl}$ (mm)	$D_{blg}$ (mm)	$D_{shaft}$ (mm)	$L_{cyl}$ (mm)	$L_{blg}$ (mm)	$L_{blgshaft}$ (mm)
4	20	17	16	68	20	6
17	54	36	30	160	20	3
19	40	27	20	100	17	3

The prementioned study in the literature uses a two-dimensional finite element model and defines the shaft and tube as analytical rigid parts.

To represent the *LEDs* more realistically, all parts of *L-LEDs* were modeled as deformable parts.

In contradistinction to the finite element model for *T-LED* which was developed by the authors and discussed in Chapter 2.2, a monotonic displacement procedure with a loading rate of 0.5 mm/sec was applied to make a better comparison with the experiment results of *L-LEDs*, Figure 10.

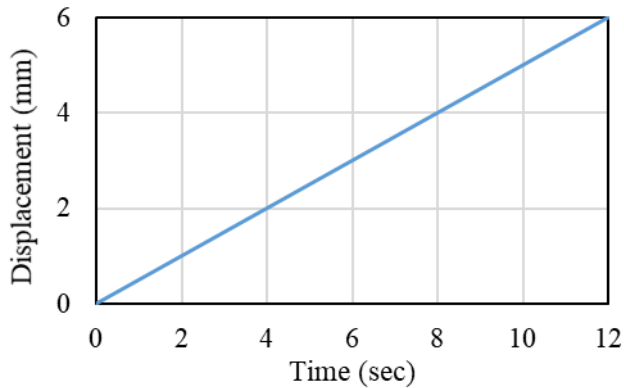


Figure 10 Ramp-type displacement procedure applied to *L-LEDs*

### 3. RESULTS AND DISCUSSION

The gap formation that occurs behind the bulge is one of the main issues with *LED*. It was satisfactorily observed by applying the cyclic displacement procedure in the developed *FEM*, Figure 11.

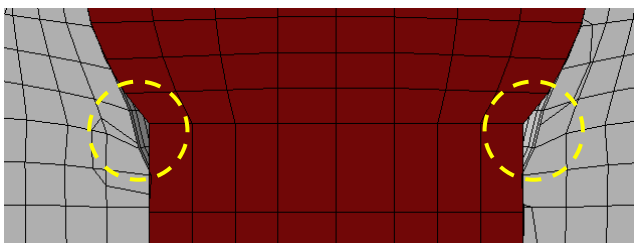


Figure 11. Gap formation at 4.5 mm (pull)

As the lead was pressurized and squeezed on one side by the movement of the shaft, out-of-plane stresses of the steel tube at that side increased, Figure 12. The highest levels of stress experienced by lead were observed to be around the shaft as expected, Figure 13. Stresses were accumulated at the front fibers of the bulge, Figure 14. All the stress distribution contours were plotted for the third cycle.

The change in the stresses observed on a mesh element in the lead throughout the analyses was plotted in Figure 15. The region of the selected finite element is shown in Figure 13. It can be stated that stress levels slightly increase with each cycle, which is also related to duration-based cumulative damage.

Steel members (tube and shaft) remained elastic even at maximum displacement levels of the shaft but plastic deformations were observed in the lead.

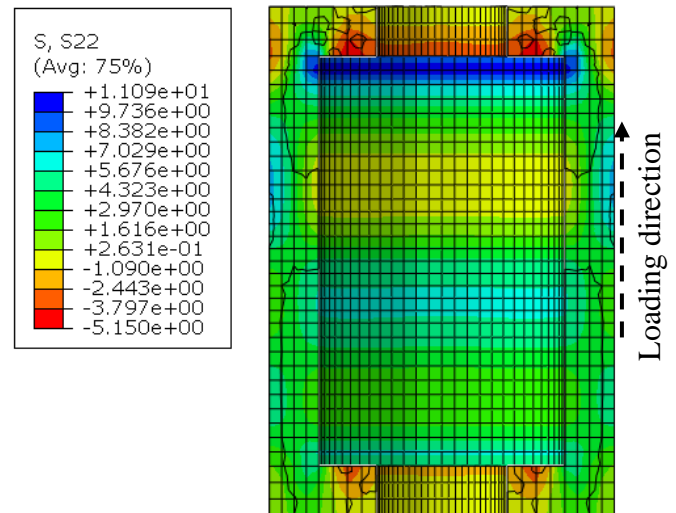


Figure 12 Stresses on the tube at 4.5 mm (pull)

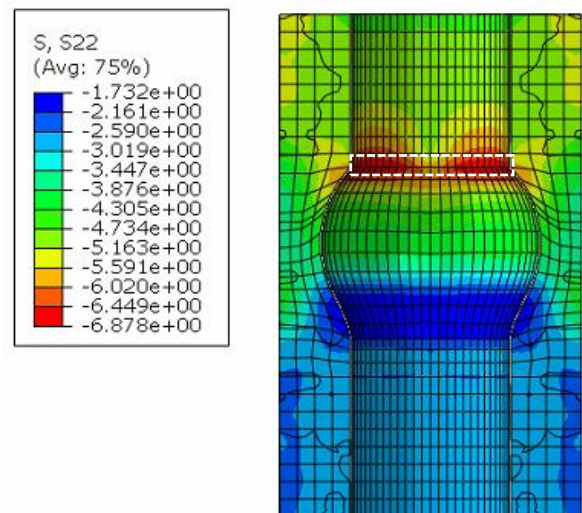


Figure 13 Stresses on the lead at 4.5 mm (pull)

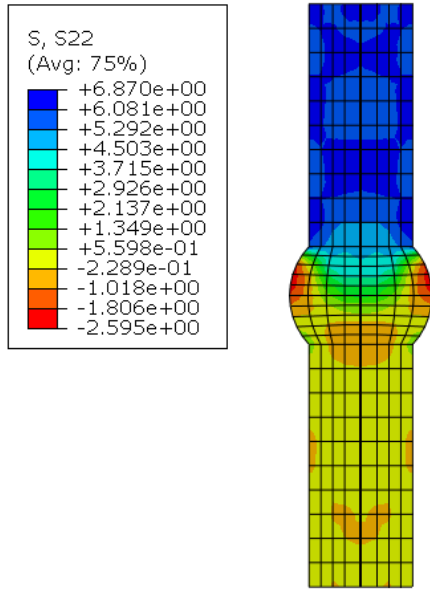


Figure 14 Stresses on the shaft at 4.5 mm (pull)

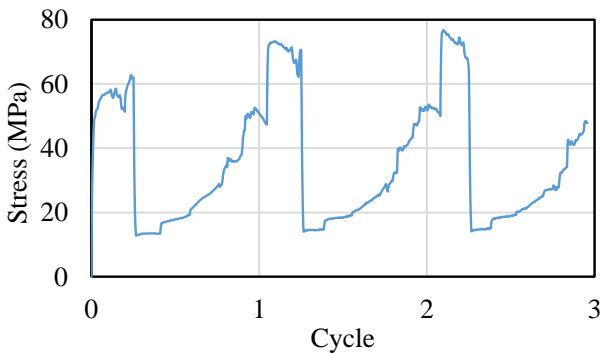


Figure 15 The change in the stress on lead.

### 3.1. Results for *T-LED*

As a result of the convergence analysis performed to investigate the mesh size effect, it was observed that the fine meshing yields better results in terms of the hysteresis shape, yield force, and maximum force values, Figure 16. Even though the computational time increases by the increasing number of mesh elements, fine meshing was selected for further analyses.

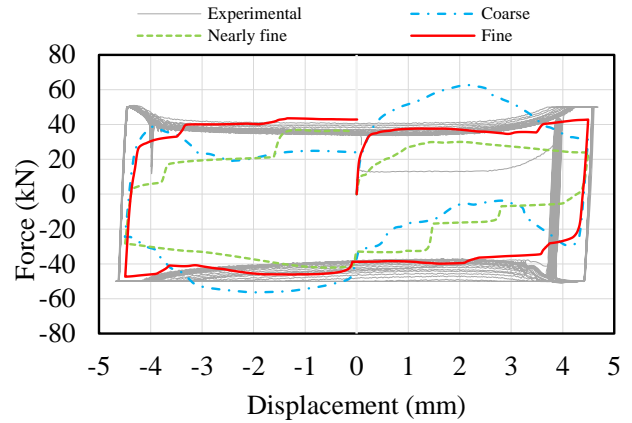


Figure 16 Convergence analysis for the mesh size

Numerically obtained force-displacement hysteresis from the preliminary *FEMs* was compared with the experimental result in Figure 17. While 30 cycles were performed in the experiments, this number was reduced to 3 cycles in numerical analyses to reduce computational time.

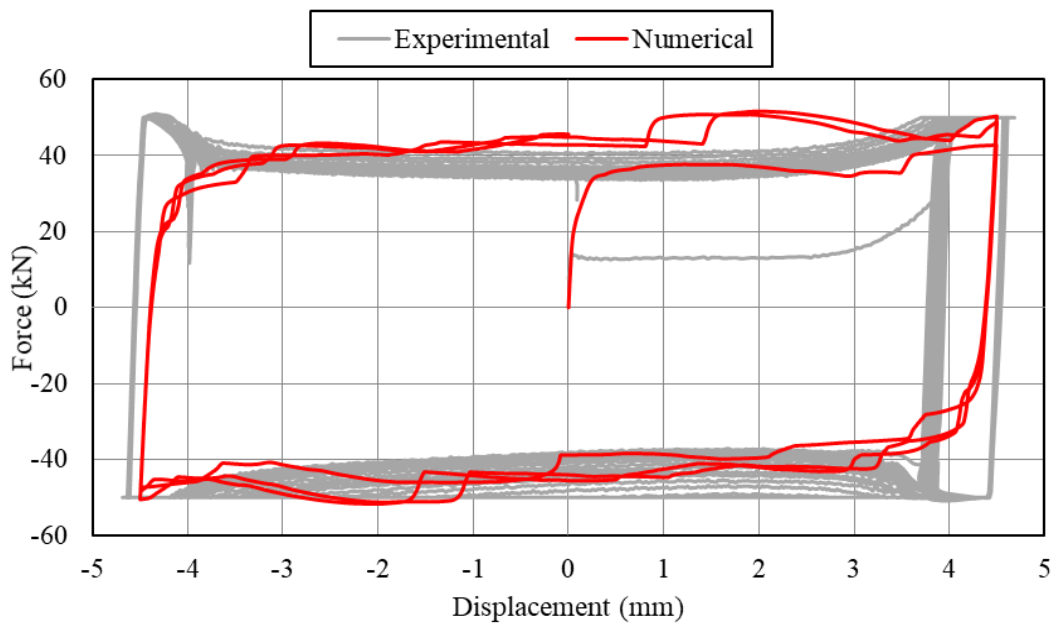


Figure 17 Comparison of experimental and numerical hysteresis of *T-LED*

Initial stiffness, force values, and loading/unloading paths were reasonably predicted by numerical analyses. Yet, there was a slight difference between experimental and numerical hysteresis. The reason for this might be the formation of air voids inside lead during the casting process. Besides, the softening of lead under repetitive cycles caused a slight decrement in yield force at each step. Air voids and softening of lead cannot be modeled through *FEMs*. Last but not the least, the mechanical properties of lead were adapted from literature.

### 3.2. Finite Element Analyses for the *L-LEDs*

In the literature study, only maximum reaction forces of *L-LEDs*, which resulted from a monotonic ramp type loading, obtained from experiments and 2D *FEAs* were compared. Hence, comparing only the maximum forces was possible in this study, also. The developed 3D *FEM* was much more efficient to predict the maximum forces.

It can be observed from Table 2 that the developed *FEM* predicts the maximum forces better. The relative difference was calculated by Equation (1). While the differences varied between 4-39% in the literature study, it was reduced to 2-12% by the developed model, Table 2.

$$Rel. Dif. = \frac{F_{num} - F_{exp}}{F_{exp}} \quad (1)$$

Table 2 Comparison of maximum forces and errors

<i>L-LED</i> #	$F_{exp}$ (kN)	Literature [21, 22]		This Study	
		$F_{num}$ (kN)	Rel. Dif. (%)	$F_{num}$ (kN)	Rel. Dif. (%)
4	85	52	39	75	12
17	200	220	-10	192	4
19	125	130	-4	123	2

## 4. CONCLUSIONS

In this study, finite element models of lead extrusion dampers (*LEDs*) were generated for numerical testing of the energy dissipating device.

The precision of the generated model was controlled by comparing the results of the geometrically updated model with the experimental results given in the literature. The following conclusions might be driven from the numerical studies:

- The gap formation behind the bulge of the shaft was satisfactorily captured by the *FEMs*. The energy dissipation capacity of the *LED* was reduced due to the existence of the gap. Developed *FEM* can be an efficient tool to reduce gap formation and enhance the performance of the *EDD*.
- Force-displacement hysteresis of the evaluated *T-LED* was successfully predicted by the developed *FEM*. The observed slight difference might be related to the air voids and softening of lead or the material properties taken from the literature.
- In the further step of the analyses, material tests will be performed on the lead, and experimentally obtained material properties will be defined in the *FEMs*.
- Air voids inside the lead should be minimized so pre-stressing can be an effective method in this regard. Pre-stressing may also be influential on gap formation behind the bulge of the shaft.
- The finite element model used in this study was shown to yield better results compared to the one used in the literature since *LEDs* were modeled more real-like (three-dimensional and deformable) in this study.

### Acknowledgments

The study was performed in the Structural and Earthquake Engineering Laboratory of Istanbul Technical University. The contribution of the laboratory staff is gratefully acknowledged.

### Research and Publication Ethics

This paper has been prepared within the scope of international research and publication ethics.

**Ethics Committee Approval**

This paper does not require any ethics committee permission or special permission.

**Conflict of Interest**

The authors declared no potential conflicts of interest with respect to the research, authorship, and/or publication of the paper.

**REFERENCES**

- [1] M. G. Soto, and H. Adeli, "Semi-active vibration control of smart isolated highway bridge structures using replicator dynamics," *Engineering Structures*, vol. 186, pp.536-552, 2019.
- [2] Y. Luo, X. Zhang, Y. Zhang, Y. Qu, M. Xu, K. Fu and L. Ye, "Active vibration control of a hoop truss structure with piezoelectric bending actuators based on fuzzy logic algorithm," *Smart Materials and Structures*, vol. 27, no.8, 085030, 2018.
- [3] X. Liu, G. Cai, F. Peng and H. Zhang, "Dynamic model and active vibration control of a membrane antenna structure," *Journal of Vibration and Control*, vol. 24, no. 18, pp. 4282-4296, 2017.
- [4] F. Karadoğan, E. Yüksel, A. Khajehdehi, H. Özkaynak, A. Güllü, and E. Şenol, "Cyclic behavior of reinforced concrete cladding panels connected with energy dissipative steel cushions," *Engineering Structures*, vol. 189, pp. 423-439, 2019.
- [5] E. Yüksel, F. Karadoğan, H. Özkaynak, A. Khajehdehi, A. Güllü, E. Smyrou and İ. E. Bal, "Behavior of steel cushions subjected to combined actions," *Bulletin of Earthquake Engineering*, vol. 16, no. 2, pp. 707-729, 2018.
- [6] H. Özkaynak, A. Khajehdehi, A. Güllü, F. Azizisales, E. Yüksel and F. Karadoğan, "Uni-axial behavior of energy dissipative steel cushions" *Steel and Composite Structures*, vol. 27, no. 6, pp. 661-674, 2018.
- [7] P. Saingam, F. Sütçü, Y. Terazawa, K. Fujishita, P. C. Lin, O. C. Çelik and T. Takeuchi, "Composite behavior in RC buildings retrofitted using buckling restrained braces with elastic steel frames," *Engineering Structures*, vol. 219, 110896, 2020.
- [8] A. Xhahysa, S. Kahraman and S. C. Girgin, "Flexure based energy dissipating device in self-centering braces," *Latin American Journal of Solids and Structures*, vol. 16, no. 8, e231, 2019.
- [9] T. T. Soong and B. F. Spencer, "Supplemental energy dissipation: state-of-the-art and state-of-the-practice," *Engineering Structures*, vol. 24, pp. 243-249, 2002.
- [10] P. Deng, Z. Gan, T. Hayashikawa and T. Matsumoto, "Seismic response of highway viaducts equipped with lead-rubber bearings under low temperature," *Engineering Structures*, vol. 209, 110008, 2020.
- [11] G. Özdemir and H. P. Gülkan, "Scaling legitimacy for design of lead rubber bearing isolated structures using a bounding analysis," *Earthquake Spectra*, vol. 32, no.1, pp. 345-366, 2016.
- [12] P. Shoaie, H. T. Orimi and S. M. Zahrai, "Seismic reliability-based design of inelastic base-isolated structures with lead-rubber bearing systems," *Soil Dynamics and Earthquake Engineering*, vol. 115, pp. 589-605, 2018.
- [13] C. Soydan, A. Güllü, O. E. Hepbostancı, E. Yüksel, and E. İrtem, "Design of a Special Lead Extrusion Damper", 15th World Conference on Earthquake Engineering, Lisboa, Portugal, September 24-28, 2012.
- [14] C. Soydan, E. Yüksel, and E. İrtem, "The Behavior of a Steel Connection Equipped

- with the Lead Extrusion Damper”, *Advances in Structural Engineering*, vol. 17, no. 1, pp. 25-40, 2014.
- [15] C. Soydan, E. Yüksel, and E. İrtem, “Determination of the characteristics of a specially designed lead extrusion damper”, 14th World Conference on Seismic Isolation, Energy Dissipation and Active Vibration Control of Structures, San Diego, USA September 9-11, 2015.
- [16] C. Soydan, “A new energy dissipating device and its application to pinned connections in precast structural systems”, Ph.D. thesis, Istanbul Technical University, Istanbul, Turkey, 2015.
- [17] C. Soydan, E. Yüksel, and E. İrtem, “Determination of the characteristics of a new prestressed lead extrusion damper”, 16th World Conference on Earthquake Engineering, Santiago, Chile, 2017.
- [18] C. Soydan, E. Yüksel, and E. İrtem, “Retrofitting of Pinned Beam–Column Connections in RC Precast Frames Using Lead Extrusion Dampers”. *Bulletin of Earthquake Engineering*, vol. 16, no. 3, pp. 1273–1292, 2017.
- [19] C. Soydan, E. Yüksel and E. İrtem, “Seismic performance improvement of single-storey precast reinforced concrete industrial buildings in use,” *Soil Dynamics and Earthquake Engineering*, vol. 135, 106167, 2020.
- [20] W. H. Robinson and L. R. Greenbank, “Properties of an extrusion energy absorber,” *Bulletin of New Zealand Society of Earthquake Engineering*, vol. 8, no. 3, pp. 187-191, 1975.
- [21] V. Vishnupriya, G. W. Rodgers, and J. G. Chase, “Finite element modelling of HF2V lead extrusion dampers for specific force capacities”, 2019 Pacific Conference on Earthquake Engineering, Auckland, New Zealand, April 4-6, 2019.
- [22] V. Vishnupriya, “Modelling force behaviour and contributions of metallic extrusion dampers for seismic energy dissipation”, Ph.D. thesis, University of Canterbury, Christchurch, New Zealand, 2019.
- [23] SIMULIA Abaqus/CAE (Version 2019) [Computer software]. Vélizy-Villacoublay: Dassault Systemes.